Journal of Molecular Structure xxx (xxxx) 131584

Contents lists available at ScienceDirect

Journal of Molecular Structure

journal homepage: www.elsevier.com/locate/molstruc

Bioactivity studies of two copper complexes based on pyridinedicarboxylic acid *N*-oxide and 2,2′-bipyridine

Hossein S. Moradi [a, 1], Elham Momenzadeh [b, 1], Monireh Asar [a, 1], Sonia Iranpour [a], Ahmad Reza Bahrami [a, c], Maryam Bazargan [b], Halimeh Hassanzadeh [a], Maryam M. Matin [a, d, *], Masoud Mirzaei [b, *]

[a] Department of Biology, Faculty of Science, Ferdowsi University of Mashhad, Mashhad 9177948974, Iran
[b] Department of Chemistry, Faculty of Science, Ferdowsi University of Mashhad, Mashhad 9177948974, Iran
[c] Industrial Biotechnology Research Group, Institute of Biotechnology, Ferdowsi University of Mashhad, Mashhad, Iran
[d] Novel Diagnostics and Therapeutics Research Group, Institute of Biotechnology, Ferdowsi University of Mashhad, Mashhad, Iran

ARTICLE INFO

Article history:
Received 13 August 2021
Received in revised form 22 September 2021
Accepted 24 September 2021

Keywords:
Copper complex
Pyridinedicarboxylic acid N-oxide
2,2′-Bipyridine
Noncovalent interactions
Combination effect
Anticancer activity

ABSTRACT

Bioactivity of two heteroleptic copper complexes based on pyridinedicarboxylic acid *N*-oxide and 2,2′-bipyridine which benefit from extensive hydrogen bonds and π-interactions are reported. Anti-cancer activities of **1** and **2** were evaluated by MTT assay against a panel of murine and human cancer cell lines. Moreover, the synergistic effects of **1** in combination with cisplatin, paclitaxel, and topotecan were investigated on HeLa cells. Cell death mechanism induced by **1** was also assessed using FITC-annexin V/PI staining. MTT results indicated that 1inhibited the proliferation of cancerous cells as compared with normal cells. Complex **2** also exerted selective toxicity towards both murine and human colon cancer cells. Moreover, the strongest synergistic effect was obtained from the combination of **1** with topotecan, and apoptosis was the main mechanism of cell death. Our results indicated that both complexes significantly inhibited the proliferation of cancerous cells. Furthermore, complex **1** can be a promising chemotherapeutic agent to be used in combination with other drugs for treatment of cervical cancer, although more studies are required to confirm this.

1. Introduction

Cancer, as a major public health problem, is the second leading cause of death and cervical cancer is the third most common malignancy among women worldwide (WHO) [1]. Chemotherapy is considered as a standard treatment for advanced, metastatic cancers and is effectively performed with platinum-based metal complexes such as cisplatin, carboplatin and oxaliplatin [2]. Despite the widespread clinical use, platinum complexes still have some side effects such as neuro-, hepato- and nephrotoxicity and also acquired drug resistance in several cancers [3,4]. Although cervical cancer can be cured, most patients suffer from side effects such as tiredness, bowel and bladder problems, lymphedema, sexual issues, infertility and temporary or permanent menopause which can increase the risk of osteoporosis and heart diseases following treatment [5,6].

These issues have led to ongoing research to discover more effective chemotherapy agents with less side effects. In the last few decades, other bio-essential metal ions such as copper have been widely investigated as antiproliferative agents [7,8]. Copper acts as an important biometal and essential cofactor in several proteins and enzymes, and it mainly functions in oxidation-reduction reactions [9]. Since it is found in all living organisms, it can be assumed that copper complexes may cause less side effects than non-essential metals such as platinum, when used as chemotherapeutic agents [10].

Apart from the metal ion, the structure of the organic ligand(s) has a great influence on the final biological properties. For example, many *O/N*-donor ligands show potential applications specially as anticancer agents [11]. In this regard, antiproliferative effects of pyridine complexes containing copper have been investigated [8]. It has been shown that antiproliferative effect of the copper bipyridine compound is concentration dependent on both human HL-60 promyelocytic leukemia and chronic myelogenous leukemia K562 cells [12]. It is well known that heteroleptic complexes, which contain more than one type of ligand, can show greater bioactivity because of the synergistic effects of the organic ligands. However, combination chemotherapy approach is

* Corresponding authors.
E-mail addresses: matin@um.ac.ir (M.M. Matin), mirzaeesh@um.ac.ir (M. Mirzaei).
[1] These authors contributed equally.

https://doi.org/10.1016/j.molstruc.2021.131584
0022-2860/

also an efficient method for cancer treatment. In this way, the effect of the combination of two or more drugs can be greater than the additive effects of those drugs [13]. In addition, synergistic therapeutic effects can increase efficacy and this can reduce the dose of the drugs; for example, assuming that two drugs show synergy, a lower dose of each would be needed to achieve the same effect and thereby decreasing the side effects, as well as drug resistance. One of the most widely used approaches for detecting and measuring the synergistic effects between drugs is Chou and Talalay method. By calculating combination index (CI) in this method, one can quantitatively describe the interactions between two or more drugs. Advantages of this method include numerical results, requirement for minimal data to assess the behavior of materials in combination, time saving, and the possibility of investigating drug interactions both *in vitro* and *in vivo* [14,15]. Apoptosis is a process of programmed cell death, which can occur through two pathways: extrinsic or death receptor pathway and intrinsic or mitochondrial pathway [16]. Studies have suggested that apoptosis can effectively suppress tumor progression. As a result, apoptosis inducing features of chemotherapeutic agents would be advantageous in cancer therapy [17]. Several reviews reflect the huge potential of metal-based frameworks as drug delivery and cancer theragnostic platforms [18,19].

Therefore, inspired by these factors, we selected pyridinedicarboxylic acid *N*-oxide, 2,2′-bipyridine ligands as well as copper to create bioactive complexes formulated as [Cu(Hpydco)(bpy)Cl]•2H_2O (**1**), and [Cu(pydco)(bpy)H_2O]•3H_2O (**2**). Furthermore, cytotoxic effects of these complexes were determined on cancerous cell lines. Then, we investigated the effects of **1** in combination with common chemotherapeutic drugs including cisplatin, paclitaxel and topotecan on HeLa cells.

2. Experimental

2.1. Materials and instruments

All chemicals and solvents were purchased from commercial sources and used without further purification, except for pyridine-2,n-dicarboxylic acid *N*-oxide (H_2pydco) which was synthesized according to a reported method [20,21]. Roswell Park Memorial Institute (RPMI 1640) medium, high glucose Dulbecco's modified Eagle's medium (HG-DMEM), fetal bovine serum (FBS) and trypsin-EDTA solution were provided from Life Technologies (UK). 3-(4,5-dimethylthiazol-2-yl)-2, 5-diphenyltetrazolium bromide (MTT), phosphate buffered saline (PBS) and dimethyl sulfoxide (DMSO) were purchased from Sigma-Aldrich (Germany). FITC-annexin V Apoptosis Detection Kit with propidium iodide (PI) was obtained from BioLegend (USA). Cisplatin (Mylan), paclitaxel (Sobhan), and topotecan (Thymoorgan Pharmazie gmbh) were kindly provided by Dr Fatemeh Homaei Shandiz (Mashhad University of Medical Sciences). Melting points were determined using a Barnstead Electrothermal 9300 apparatus. The infrared spectra were recorded in the range of 4000–400 cm^{-1} on a Thermo Nicolet/AVATAR 370 Fourier transform spectrophotometer using KBr pellets. Elemental analysis (CHN) was performed using a Thermo Finnigan Flash-1112 EA microanalyzer. Single crystal X-ray diffraction data were obtained using a Bruker Smart APEX diffractometer. The optical density (OD) of the cells was measured using an enzyme-linked immunosorbent assay (ELISA; Awareness Technology, USA). The mechanism of cell death was determined using BD Accuri C6 flow cytometer (Becton Dickinson, USA).

2.2. Synthesis and characterization

2.2.1. Synthesis of 1

The synthetic procedure and structure of **1** were reported previously by some of us [22]. Generally, a solution of bpy (0.078 g, 0.50 mmol), pyridine-2,5-dicarboxylic acid *N*-oxide (0.092 g, 0.50 mmol) and $CuCl_2$•2H_2O (0.085 g, 0.50 mmol) in ethanol–water (1: 1; 25 mL) was stirred at room temperature for 4 h. After 14 days, green crystals were obtained by slow evaporation from the reaction mixture at room temperature in 52% yield (based on Cu) (m.p. 244 °C). Anal. Calcd (%) for $C_{17}H_{16}CuN_3O_7Cl$: C, 46.72; H, 3.11; N, 9.61. Found: C, 46.42; H, 3.19; N, 9.26. IR bands (KBr pellet, cm^{-1}): 3505, 3071, 1741, 1652, 1567, 1392, 1341, 1205.

2.2.2. Synthesis of 2

A solution of of bpy (0.032 g, 0.20 mmol), pyridine-2,6-dicarboxylic acid *N*-oxide (0.018 g, 0.10 mmol) and $CuCl_2$•2H_2O (0.01 g, 0.05 mmol) in 9 mL of water was stirred at 50 ºC for 3 h. After 13 days, blue crystals were obtained by slow evaporation from the reaction mixture at room temperature in 45% yield (based on Cu) (m.p. 197 °C). Anal. Calcd (%). for $C_{17}H_{17}CuN_3O_8$: C, 43.18; H, 4.07; N, 8.89. Found: C, 43.53; H, 4.01; N, 9.16. IR bands (KBr pellet, cm^{-1}): 3427, 1604, 1368, 1234.

2.3. X-ray structure determination

Crystal and refinement details are presented in supplementary Table S1. The diffraction data were collected under control of the APEX3 software [23,24] and reduced to F^2 values with SAINT [24]. Analytical absorption corrections and merging of equivalent reflections was performed with SADABS [25] and the structures solved by dual space methods (SHELXT [26]). The structures were refined by full-matrix, least-squares methods (SHELXL [27]) and hydrogen atoms attached to carbon were included as riding contributions in idealized positions with isotropic displacement parameters tied to those of the attached atoms. Where possible, hydrogen atoms attached to water molecules were placed so as to maximize hydrogen bonding interactions and similarly included as riding contributions.

2.4. Preparing different solutions of 1 and 2

In order to prepare different concentrations (6.25, 12.5, 25, 50, and 100 μgmL^{-1}) of **1** and **2**, 2 mg of powder was dissolved in 100 µL distilled water and then diluted with complete culture medium before treatments. In order to eliminate the effects of solvent and evaluate the absolute effects of different concentrations, the viability of each treatment group was compared with its control containing equal amounts of solvent.

2.5. Cell culture

CT26, a mouse colon carcinoma cell line, 4T1 cells, mouse stage IV breast cancer cells and HeLa, a human cervical cancer cell line, were purchased from Pasteur Institute (Tehran, Iran). LoVo, a human colon carcinoma cell line, was received as a gift from Dr. Maite Huarte (University of Navarra, Spain). C26, a mouse colon carcinoma cell line, was purchased from Cell Lines Service (Eppelheim, Germany). TUBO cells, derived from mouse mammary gland tumor, was kindly provided by Dr. Pier-Luigi Lollini (Department of Clinical and Biological Sciences, University of Turin, Orbassano, Italy) and HDF, human dermal fibroblast cells, were a generous gift from Royan Institute (Tehran, Iran).

CT26, C26, 4T1, LoVo and HeLa cells were cultured in RPMI 1640 medium, supplemented with 10% (v/v) FBS. TUBO and HDF cells were cultured in HG-DMEM supplemented with 20% and 10% (v/v) FBS, respectively. All cell lines were maintained at 37 °C in a humidified atmosphere containing 5% CO_2. Cells were passaged with 0.25% trypsin and 1 mM EDTA solution when required.

2.6. Cell viability assay

Cytotoxicity was measured by MTT assay [28]. In this method, CT26 (1.3×10^4 cells / well), C26 (1.3×10^4 cells / well), 4T1 (0.8×10^4 cells / well), LoVo (0.6×10^4 cells / well), TUBO (1.3×10^4 cells /

well), HeLa (1.2×10^4 cells / well) and HDF cells (0.8×10^4 cells / well) were seeded in 96-well plates. After 24 h incubation when confluency reached 70–80%, cells were treated with different concentrations of **1** or **2**. To evaluate cytotoxicity after 24, 48 and 72 h, 20 μL MTT dye (5 $mgmL^{-1}$ in PBS) was added to each well and cells were incubated at 37 °C for 4 h. The supernatants were then aspirated carefully and resulting formazan crystals were dissolved in 150 μL DMSO and the absorptions were measured at 545 nm wavelength by an ELISA reader.

2.7. Drug combination studies

IC_{50} for drugs were calculated using cell viability assay as described above (section 2.6.). Cisplatin, topotecan (15.62, 31.25, 62.5, 125, 250, 500, and 1000 μgmL^{-1}) and paclitaxel (93.75, 187.5, 375, 750, 1500, 3000, and 6000 μgmL^{-1}) were dissolved in distilled water and diluted in culture media before use. HeLa cells were seeded in 96-well plates and treated with each drug. The IC_{50} values obtained from each drug cell viability assay were used to design subsequent drug combination experiments. In order to evaluate combination effects, several concentrations lower and higher than IC_{50} values were selected and then interactions between **1** and chemotherapeutic drugs were assessed, at a constant concentration ratio. Used concentration ranges, and **1** to drug molar ratios are shown in Tables 1–3. To determine the nature of drug interaction (synergism, additive or antagonism), data were analyzed by median effect methods using the Compusyn software developed by Chou and Talalay. In this method using CI allows quantitative determination of drug interaction in which CI < 1 indicates synergistic activity; CI = 1, additive and CI > 1 determines antagonism [14].

2.8. Identification of apoptosis by FITC-annexin V/PI staining

Apoptotic cell death was quantified using the FITC-annexin V Apoptosis Detection Kit with PI. For this purpose, HeLa cells were seeded at a density of 3.8×10^5 cells per well in 6-well plates. After 24 h of incubation, cells were treated with ~50 μM concentration of **1** for 16 h. According to the manufacturer's instructions, cells were collected by centrifugation and washed twice with cold cell staining buffer and then resuspended in binding buffer at a concentration of 1×10^6 cells/mL. 100 μL of cell suspension were then incubated with 5 μL of FITC-annexin V and 10 μL PI for 15 min at room temperature in the dark, followed by diluting cell suspension in 400 μL binding buffer. Samples were analyzed using the BD Accuri C6 flow cytometer and analyzed using FlowJo V.7.6 software.

Table 1
Concentration ranges of **1** and cisplatin, and their constant molar ratios used in combination.

Time (h)	Concentration range of **1** (μM)	Cisplatin concentration range (μM)	Complex **1** -to-cisplatin ratio
24	9 –119	3.98–52.65	2.2
48	2–112	0.44–24.89	4.5
72	5–90	1.61–29.03	3.1

Table 2
Concentration ranges of **1** and paclitaxel, and their constant molar ratios used in combination.

Time (h)	Concentration range of **1** (μM)	Paclitaxel concentration range (μM)	Complex **1** -to-paclitaxel ratio
24	9–129	2.67–38.27	3.3
48	2–112	0.55–31.11	3.6
72	5–95	0.92–17.59	5.4

Table 3
Concentration ranges of **1** and topotecan, and their constant molar ratios used in combination.

Time (h)	Concentration range of **1** (μM)	Topotecan concentration range (μM)	Complex **1** -to-topotecan ratio
24	3–119	12.09–479.83	0.24
48	2–102	8.43–430.37	0.23
72	1–90	3.74–337.07	0.26

2.9. Statistical analysis

MTT results were normalized to control, and the IC_{50} values were calculated by non-linear regression analysis using the GraphPad Prism 6.07 software. Data are expressed as mean ± SEM or SD as indicated in each case. Statistical comparisons were based on unpaired *t* test and *P*-values ≤ 0.05 were considered as significant.

3. Structural studies

3.1. Synthesis

As an extension of our interest in pyridine-dicarboxylic acid *N*-oxides [22,29–35], we utilized them in the design and synthesis of two new complexes. In this regard, **1** and **2** were synthesized by the reaction of copper ion, pyridine-2,n-dicarboxylic acid *N*-oxide (n: 5 and 6; H_2pydco), and bpy at ambient temperature (see the Experimental Section for details). Careful control of reaction time and solvent type are key factors to obtain the complexes reported herein. The crystallization time for **1** and **2** was a few days by slow evaporation of mother liquor.

3.2. IR spectra

The infrared spectra of **1** and **2** are consistent with the structures determined by single-crystal X-ray diffraction (supplementary Figs S1 and S2). The broad and strong bands at 3000–3500 cm^{-1} can be attributed to the O–H stretching vibrations of lattice and coordinated water molecules. They are also indicative of the presence of hydrogen bonds. Moreover, characteristic strong bands for the coordinated carboxylate groups of the $Hpydco^-$ and $pydco^{2-}$ are seen in the ranges 1604–1643 and 1368–1398 cm^{-1}, for the asymmetric and symmetric stretching vibrations, respectively. The separation between $\upsilon_{as}(COO^-)$ and $\upsilon_s(COO^-)$ has been often used to diagnose the coordination modes for carboxylate ligands. The separation for monodentate carboxylate groups is > 200 cm^{-1}, whereas it is > 200 cm^{-1} in bidentate ones. In our complexes this separation showed that the carboxylate group is coordinated monodentately to the metal center in agreement with the crystal structure. Bands in the 1206 and 1221 cm^{-1} region were assigned to the N–O stretching vibrations of the pyridine-*N*-oxide. Furthermore, the strong absorption bands in the range of 1550–1600 cm^{-1} can be attributed to the C=C and C=N vibration of aromatic pyridyl ring [36].

3.3. Structure description

Single-crystal X-ray diffraction data, data collection, and structure refinement details are summarized in supplementary Table S1. Crystallographic details can be found in the CIF files. The CIF files are available free of charge from the Cambridge Crystallographic Data Centre CCDC (1554226 and 1861390). Structural analysis indicates that **1** and **2** contain discrete complexes containing *N*-donor bpy and *O*-donor $pydco^{2-}$ (or $Hpydco^-$) ligands. The copper centers in **1** and **2** adopted distorted square pyramidal coordination geometry (Fig. 1). Selected bond distances and angles and a list of hydrogen bond geometries are reported in supplementary Tables S2 and S3 (in the Electronic Supplementary Material (ESM†)).

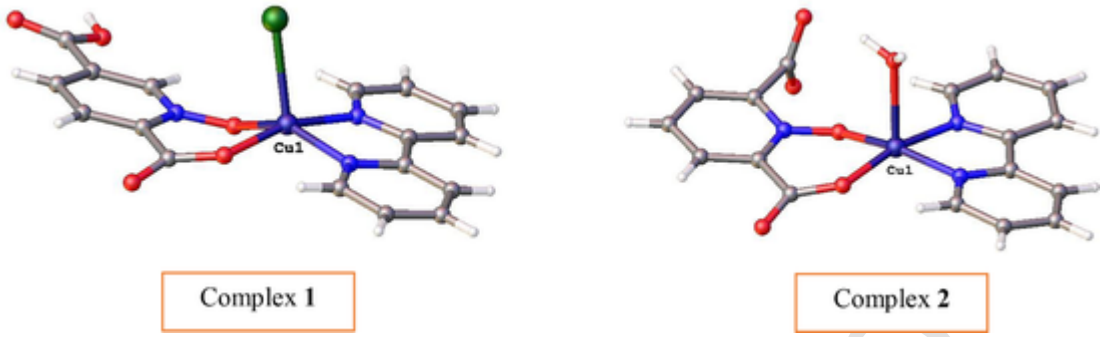

Fig. 1. The asymmetric units of **1** and **2** (uncoordinated water molecules are omitted for clarity). Color codes: C, grey; N, blue; O, red; H, white.

3.4. Crystal structure of 2

Complex **2** has a monomeric structure with the $[Cu(pydco)(bpy)H_2O]\bullet 3H_2O$ formula. The asymmetric unit of **2** is composed of one Cu(II) ion, one $pydco^{2-}$ and one bpy ligand (Fig. 1). The copper center displays distorted square pyramidal coordination geometry in which the axial position is occupied by O_{water}, and the equatorial positions are occupied by N2 and N3 from the bpy ligand as well as O3 and O5 atoms of $pydco^{2-}$ ligand (Fig. 1). As shown in Fig. 2, π-interactions between aromatic rings are excellent structural-directing agents that link neighboring monomers to each other to create 2D-supramolecular layers in the *ab* plane (d_{center} = 3.762 Å and d_{plain} = 3.281 Å and the α angle is 29.541°; d_{center} = 3.598 Å and d_{plain} = 3.307 Å and the α angle is 23.219°; $d_{CH\bullet\bullet\bullet center}$ = 3.261 Å and d_{plain} = 3.115 Å and the α angle is 17.253°; $d_{CH\bullet\bullet\bullet center}$ = 3.207 Å and d_{plain} = 3.176 Å and the α angle is 8.109°). Furthermore, intermolecular hydrogen bonds can connect these layers to create a 3D-supramolecular architecture (O–H•••O and C–H•••O hydrogen bonds between the uncoordinated water molecules as well as carboxylate groups) (supplementary Fig. S3).

4. Biological studies

4.1. Investigation anticancer potential of complex 1 in vitro

4.1.1. Complex 1 exhibited significant toxicity against murine colon and breast cancer cells

To investigate *in vitro* cytotoxic effects of **1** on murine cancerous cells, CT26, C26, TUBO and 4T1 cell lines were treated with different concentrations of this complex and cell viabilities were determined by MTT assay after 24, 48 and 72 h of treatments. Dose-response curves were plotted (Fig. 3 a–d) and the IC_{50} values were calculated as shown in Table 4. Interestingly, **1** exhibited a dose- and time-dependent toxicity with cytotoxic effects on all cells including, CT26, C26, TUBO and 4T1 cells and the IC_{50} values were calculated as 19 μg mL^{-1} (40 μM), 22 μgmL^{-1} (47 μM), 11 μg mL^{-1} (24 μM) and 11 μgmL^{-1} (24 μM) after 72 h of treatments, respectively.

4.1.2. Complex 1 has anticancer effects on human cervical cancer cells

Since complex **1** showed a significant toxicity on murine cancerous cells, in order to further investigate its antitumor properties, we examined the effects of **1** on proliferation of HeLa cervical cancer cells and HDF normal cell line using MTT assay. For this purpose, HeLa and HDF cells were treated with increasing concentrations of **1** and cell viabilities and IC_{50} values were assessed at various time points. As depicted in Figs. 3e, **1** had a significant toxicity on HeLa cells and revealed a dose- and time-dependent decrease in cell viability. IC_{50} values were calculated as 24 μgmL^{-1} (51 μM) after 24 h, 14 μgmL^{-1} (29 μM) after 48 h and 13 μgmL^{-1} (27 μM) after 72 h of treatments (Table 4).

In order to investigate the anticancer effects and selective cytotoxicity of this complex, cell viabilities of HDF normal cells were also determined after treatment with similar concentrations of **1**. MTT assay results revealed that **1** had no significant cytotoxic activity on normal cells and the IC_{50} values were calculated as 95 μgmL^{-1} (202 μM), 55 μgmL^{-1} (126 μM) and 49 μgmL^{-1} (103 μM) after 24, 48 and 72 h of treatments, respectively (Table 4). Comparing IC_{50} values of **1** on the two cell lines indicated a significant difference and thus selective toxicity of this compound on cancerous cells in all three time points.

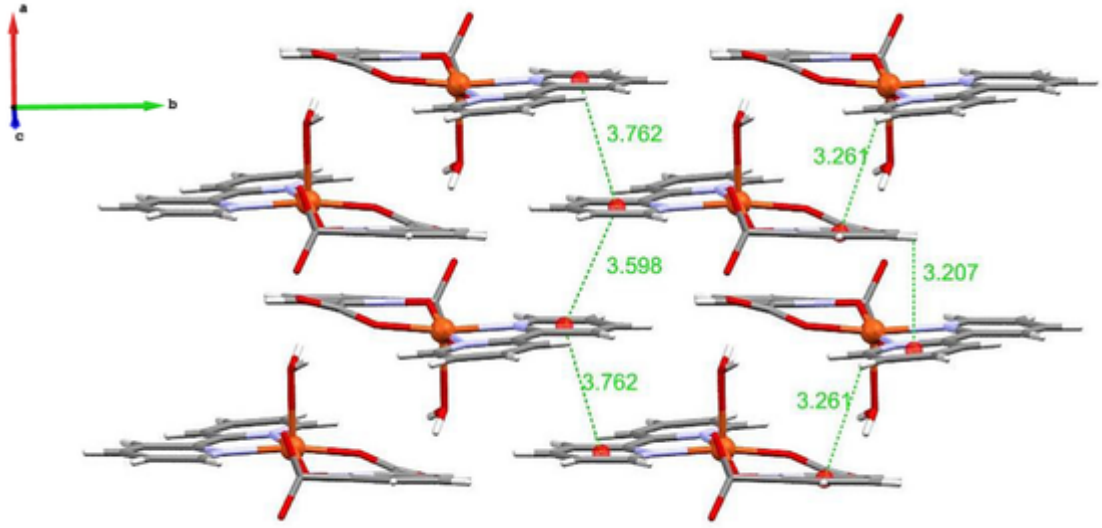

Fig. 2. 2D representation of **2** in the *ab* plane formed by π-interactions (distances are shown in Å).

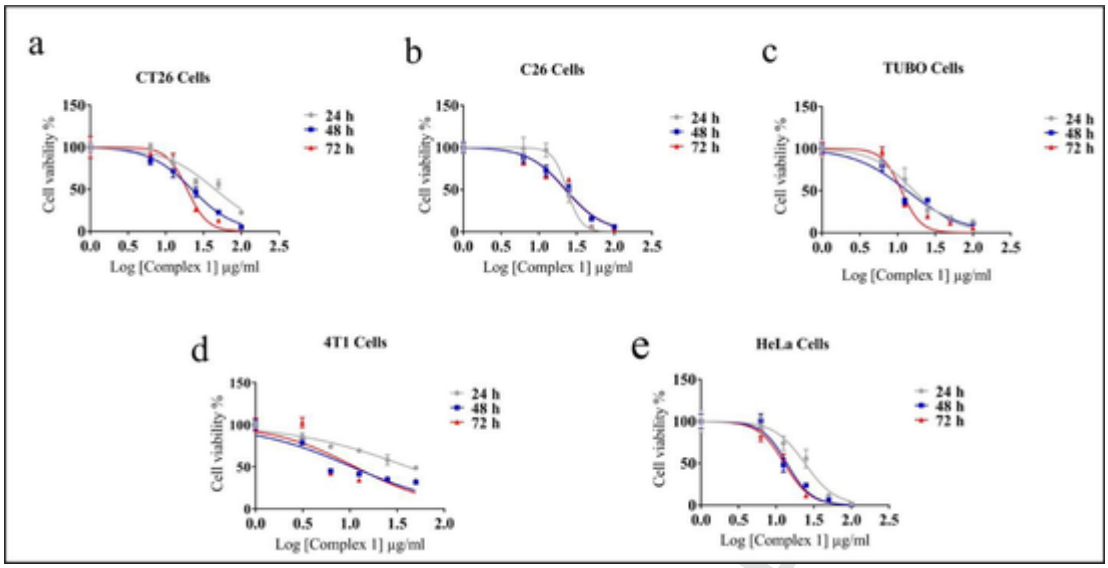

Fig. 3. Dose-response curves related to cancerous cells as determined by MTT assay. CT26 (a), C26 (b), TUBO (c), 4T1 (d) and HeLa cells (e) treated with **1** after 24, 48 and 72 h treatments. Data represent mean ± SEM (n = 3).

Table 4
Cytotoxic effects of **1** on cancerous and normal cells, as calculated by MTT assay. The IC_{50} values are shown as mean ± SD (n = 3).

Cell lines	IC_{50} (µM) ± SD		
	24 h	48 h	72 h
CT26	94.98 ± 4.28	46.73 ± 3.83	40.52 ± 3.92
C26	50.05 ± 3.73	48.17 ± 3.91	47.32 ± 4.40
TUBO	34.82 ± 2.33	28.352 ± 4.42	23.81 ± 4.11
HeLa	50.70 ± 3.93	29.28 ± 4.05	27.02 ± 3.82
HDF	202.27 ± 4.71	125.63 ± 2.46	102.93 ± 4.18

Morphological changes induced by **1** were also evaluated using an inverted microscope (HP, Japan) at different time points. Observations revealed that cells gradually lost their specific morphology and acquired a round and granulated shape which are characteristics of apoptotic cell death [37]. It is notable that similar morphological changes were observed in cisplatin treated HeLa cells (Fig. 4).

4.2. Investigating anticancer potential of complex 2 in vitro

The anticancer potential of **2** was also evaluated by MTT assay on two mouse and human colon carcinoma cell lines. Complex **2** exhibited dose- and time-dependent inhibition of cell proliferation in C26 and LoVo cells (Fig. 5). As shown in Table 5, the IC_{50} values for **2** were found to be 26.1 μgmL^{-1} (57.62 µM), 36.05 μgmL^{-1} (79.25 µM), and 600.1 μgmL^{-1} (1319.25 µM) in C26, LoVo and HDF cells after 72 h of treatments, respectively. Interestingly, significant differences ($P < 0.0001$) were observed between the cytotoxic effects of **2** on both cancerous and normal cells.

4.3. Complex 1 inhibited the proliferation of HeLa cells synergistically in combination with cisplatin, paclitaxel and topotecan

The cytotoxicity of chemotherapy drugs was first determined individually on HeLa cells. As expected, these drugs exhibited dose- and time-dependent cytotoxic effects on these cells (Table 6).

In order to investigate possible synergistic cytotoxicity of **1** and chemotherapeutic agents, the multiple drugs effect analysis method of Chou and Talalay was used. Using CI in this method can quantitatively describe the interactions between two or more drugs. Dose-response curves and F_a-CI plots (Figs. 6–8) that indicate the interactions between **1** and different drugs are described below (sections 4.3.1, 4.3.2, and 4.3.3). Moreover, the range of CI values for the three combinations is shown in Table 7.

4.3.1. Interaction between complex 1 and cisplatin

Treatment of HeLa cells with a combination of **1** and cisplatin resulted in a CI value equal to 0.42, which represents a good synergistic effect. Although in low concentrations (F_a = 50) additive interactions were observed, at high concentrations for all time intervals, CI values were consistently less than 1 and the synergy effects increased, so that the greatest synergistic effect was observed at 72 h (Fig. 6) in which CI value was calculated as 0.42 in IC_{95}. Dose reduction index (DRI) at this time ranged between 2.11–5.42 folds for **1** and 1.87–4.24 folds for cisplatin which again imply a reduced dose and synergy effect at high concentrations.

4.3.2. Interactions between complex 1 and paclitaxel

The interactions between **1** and paclitaxel were also assessed. Similar to **1** and cisplatin cotreatment, at high concentrations (F_a = 95), CI was less than 1 and synergistic effects were observed. However, in contrast to cisplatin, the greatest synergy effect was noticed at 24 h (Fig. 7) in which CI value was equal to 0.33. Moreover, DRI ranged between 1.75–3.84 folds and 3.99-13.66 folds for **1** and paclitaxel, respectively.

4.3.3. Interaction between complex 1 and topotecan

The combination of **1** with topotecan resulted in CI values of 0.75, 0.24, and 0.22 after 24 h, 48 h, and 72 h treatments, respectively. Unlike cisplatin and paclitaxel, the most synergistic effect was observed at low concentrations, while at high concentrations significant antagonistic effects (especially at 72 h) were seen (Fig. 8). According to Table 7 and similar to cisplatin, the highest synergistic effect was shown at 72 h and DRI ranged between 16–0.23 folds for **1** and 6.3–1.17 folds for topotecan.

4.4. Quantification of apoptotic cells by FITC-annexin V/PI staining and flow cytometry

Flow cytometry with FITC-annexin V/PI staining was used to study cell death mechanism induced by **1** with anticancer properties. Annexin V binds to phosphatidylserines, which during early apoptosis translocate to the extracellular leaflet and help to identify apoptotic cells. PI binds to DNA in cells in which the integrity of cell membrane is lost.

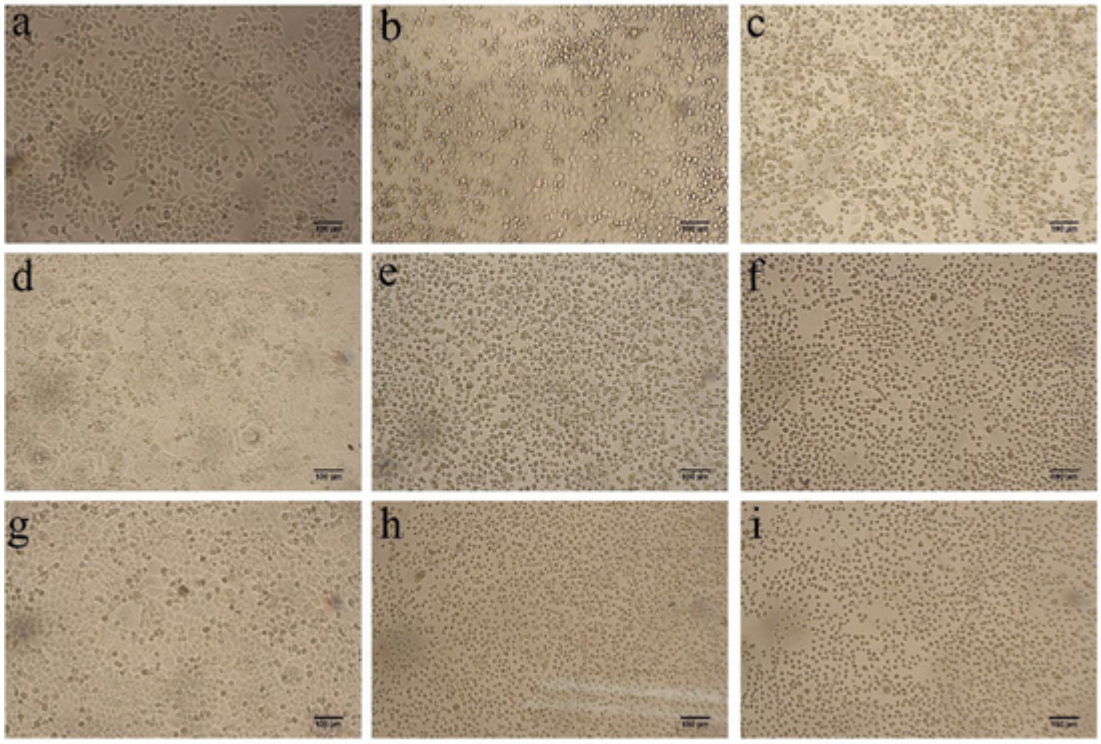

Fig. 4. Investigating morphological changes of HeLa cells. The morphology of HeLa cells without any treatment (a, d, g), treated with 25 μgmL^{-1} of 1 (b, e, h) and 25 μgmL^{-1} cisplatin (c, f, i) for 24 (a–c), 48 (d–f) and 72 h (g–i). The scale bar represents 100 μM.

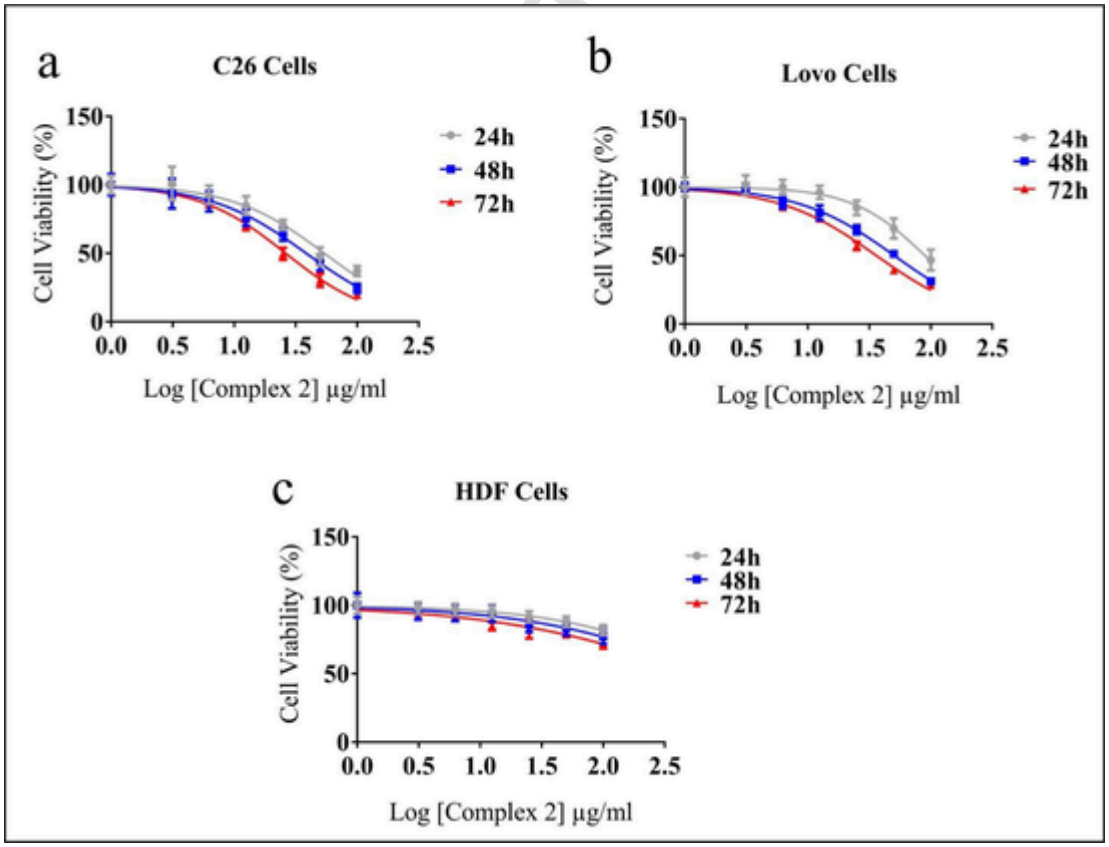

Fig. 5. Dose-response curves of **2** related to cancerous and normal cells as determined by MTT assay. Selective toxicity of **2** on C26 (a) and LoVo cells (b) in comparison with HDF cells (c), during 24, 48, and 72 h time intervals. Data represent mean ± SEM (n = 3).

Table 5
The cytotoxicity of **2** on cancerous and normal cells as calculated by MTT assay. The IC_{50} values are shown as mean ± SD, (n = 3).

Cell lines	IC_{50} (μM) ± SD		
	24 h	48 h	72 h
C26	118.75 ± 1.82	84.63 ± 1.75	57.62 ± 1.78
LoVo	197.28 ± 1.76	110.77 ± 1.78	79.25 ± 1.81
HDF	1863.82 ± 1.90	1625.95 ± 2.3	1319.27 ± 2.5

Table 6
IC_{50} values (μM) of single drugs on HeLa cells as calculated by MTT assay after 24 h, 48 h, and 72 h of treatments. The IC_{50} values are shown as mean ± SD (n = 3).

Time (h)	IC_{50} (μM) ± SD		
	Cisplatin	Paclitaxel	Topotecan
24 h	58.59 ± 6.06	17.54 ± 2.14	-
48 h	36.59 ± 6.2	6.54 ± 2.14	-
72 h	18.18 ± 6.4	4.33 ± 2.2	202.63 ± 4.72

Therefore, healthy cells are double negative, necrotic cells and cells at late stages of apoptosis are double positive for both dyes and early apoptotic cells are positive for FITC-annexin V and negative for PI [38]. As shown in Fig. 9, two-dimensional dot plots of FITC-annexin V versus PI indicate that apoptosis was induced by **1** in HeLa cells similar to cisplatin.

4.5. Discussion

Cancer is a group of diseases characterized by uncontrolled growth and spread of abnormal cells. Chemotherapy is considered as the major treatment in metastatic and advanced stages of cancer (American Cancer Society). Despite a great progress in drug development, treatment regimen is still not satisfactory and further research on new compounds is still needed for cancer therapy. Throughout history, metal complexes have been used for treatment of various diseases [39] and after discovery of cisplatin in 1960s, increasing interest was attracted towards these compounds for cancer treatment [40]. However, use of cisplatin in curative therapy is associated with acquired resistance in several types of cancers as well as significant side effects such as nephrotoxicity, hepatotoxicity and cardiotoxicity [41,42]. These disadvantages emphasize the need for development of novel non-platinum metal complexes, for which considerable progress has been made to date [4].

Several studies have shown anticancer properties of pyridine-based complexes framework [8]. Efthimiadou *et al.* showed antiproliferative effects of a copper complex of 2,2′-bipyridine on human HL-60 and K562 cells [12] Kamatchi and colleagues demonstrated anticancer properties of ruthenium complexes of 4-hydroxy-pyridine-2,6-dicarboxylic acid and 2,2′-bipyridine-5,5′-dicarboxylic acid on cancer cell lines including HeLa, HepG2 and HEp-2 in comparison with NIH-3T3 normal cells [43,44].

In general, the type and number of bound ligands surrounding the complex can be effective on biological activity of a metal complex. Bidinate carboxylate ligands have been used in cisplatin derivatives because of their high aqueous solubility and hydrolysis resistance [45]. Moreover, it has also been proved that an appropriate carboxylation in coordination complexes could modulate the solubility of the complex, cell transport, anticancer and antioxidant activities [46,47].

These studies prompted us to test possible anticancer effects of two complexes containing copper, pyridine-2,n-dicarboxylic acid *N*-oxide (n = 5 in **1** and n = 6 in **2**) and 2,2′-bipyridine on several cancerous cell lines and results revealed their concentration-dependent antiproliferative effects (Figs. 3 and 5). The anticancer proprieties of **1** were evaluated by comparing its IC_{50} values on HeLa and normal cell as presented in Table 4. Moreover, the antiproliferative potential of **2** against C26 and LoVo cells was compared with HDF cells (Table 5). It was found that **1** and **2** appeared to be potent agents, as they had selective toxicity on murine and human cancerous cells, while they had no significant antiproliferative activity on normal cells. The low toxicity of **1** and **2** on normal cells is likely due to intrinsic properties of copper. Copper is an essential endogenous metal which participates as a necessary cofactor in several enzymes and proteins such as cytochrome oxidase, superoxide dismutase, and tyrosinase. Moreover, it has been suggested that copper complexes may cause fewer side effects than non-essential metals such as platinum when used as chemotherapeutic agents [9,10]. Flow cytometry analysis showed that **1** induced cell death in HeLa cells *via* apoptosis, which was in agreement with observed morphological changes after treatment with both pyridyl carboxylate complex containing copper and cisplatin (Figs. 4 and 9).

Most cancers have multiple genetic alterations and thus a combination of drugs is usually used to have a better outcome [48]. In the pre-

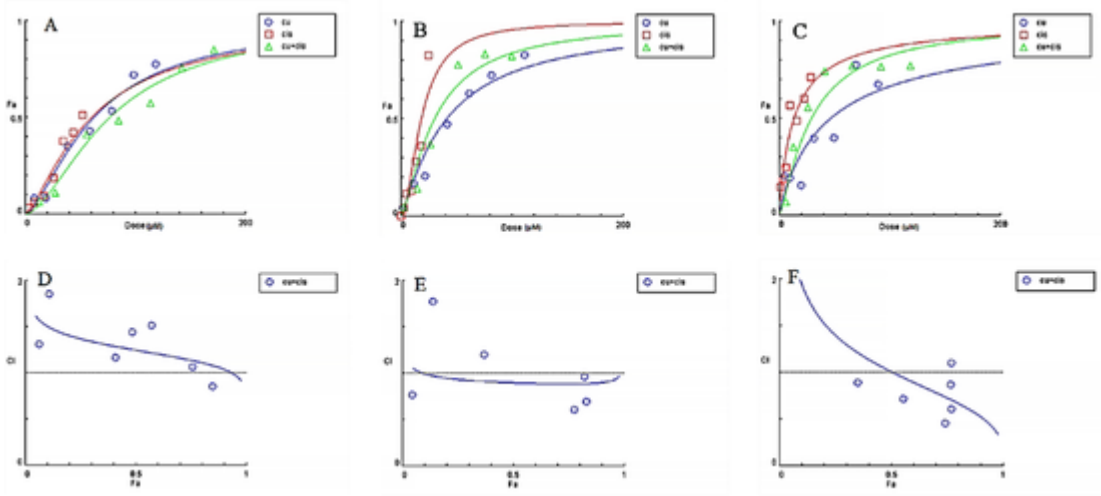

Fig. 6. Dose-response curves (A, B, C) and F_a-CI plots (D, E, F) for evaluating the effects of 1 and cisplatin combination on HeLa cells at 24 (A, D), 48 (B, E), and 72 h (C, F). Complex 1 and cisplatin alone and in combination were investigated in dose-response curves. The red, blue, and green curves are related to effects of different concentrations of cisplatin, 1 and cisplatin-complex 1 on HeLa cells, respectively, also the average r-value for drugs combination is 0.95. F_a-CI plots were generated to determine the extent of synergy for drugs combination and synergistic effects are defined as CI < 1. According to the graphs, synergistic effects can be observed in some concentrations, especially at high doses.

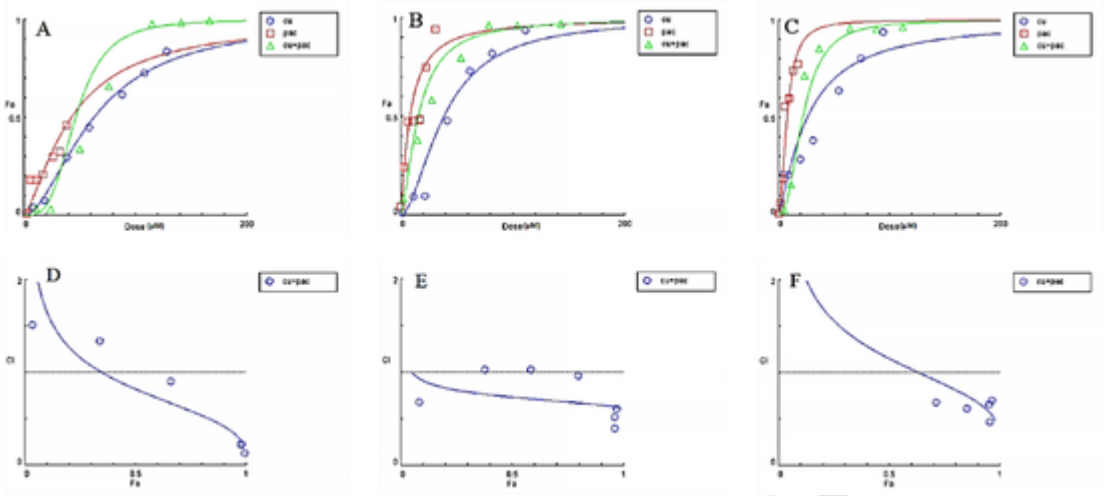

Fig. 7. Dose-response curves (A, B, C) and F_a-CI plots (D, E, F) for evaluating the effects of 1 and paclitaxel combination on HeLa cells at 24 (A, D), 48 (B, E), and 72 h (C, F). On dose-response curves, 1 and paclitaxel alone and in combination were investigated. The red, blue, and green curves are related to effects of different concentrations of paclitaxel, 1 and paclitaxel-complex 1 on HeLa cells, respectively, also the average r-value for drugs combination is 0.96. F_a-CI plots were generated to determine the extent of synergy for drugs combination and synergistic effects are defined as CI < 1. According to the graphs, synergistic effects could be observed in most concentrations for all time points especially at 24 h.

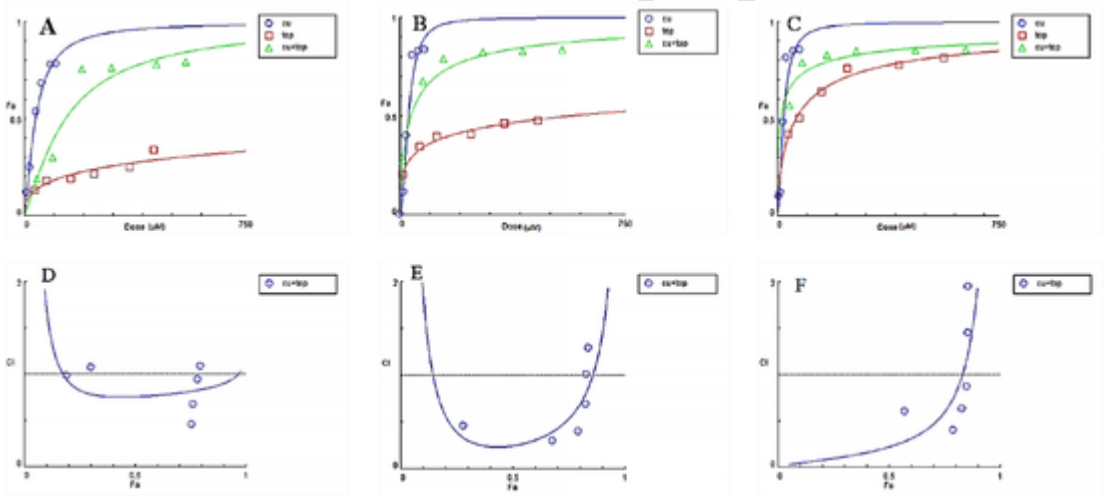

Fig. 8. Dose-response curves (A, B, C) and: F_a-CI plots (D, E, F) for evaluating the effects of 1 and topotecan combination on HeLa cells at 24 (A, D), 48 (B, E), and 72 h (C, F). On dose-response curves, 1 and topotecan alone and in combination were investigated. The red, blue, and green curves are related to effects of different concentrations of topotecan, 1 and topotecan-complex 1 on HeLa cells, respectively, also the average r-value for drugs combination is 0.93. F_a-CI plots were generated to determine the extent of synergy for drugs combination and synergistic effects are defined as CI < 1. According to the graphs, at low concentrations the two drugs show synergistic effects.

Table 7
The range of CI values in F_a 0.5 to F_a 0.95 at different times. At high F_a (F_a = 0.95), the combination of drugs had synergistic effects, except for topotecan, which at F_a 0.95 had antagonistic effects (CI = 5.09).

Drug combination	24 h	48 h	72 h
complex **1**-cisplatin	1.24–0.97	0.89–0.92	1–0.42
complex **1**-paclitaxel	0.82–0.33	0.73–0.63	1.15–0.57
complex **1**-topotecan	0.75–0.96	0.24–2.9	0.22–5.09

sent study, the effects of **1** in combination with chemotherapy drugs (cisplatin, paclitaxel, and topotecan) were analyzed using Chou-Talalay method, which is based on the median-effect equation derived from the mass-action law principle. This method is considered as the unified theory for the Michaelis-Menten equation, Hill equation, Henderson-Hasselbalch equation and Scatchard equation. These equations provide the theoretical basis for the resulting combination index (CI) equation, a quantitative definition for synergism when CI < 1, antagonism when CI > 1 and additive effects when CI = 1 [14]. For this purpose, first IC_{50} values of each drug on HeLa cells were calculated (Table 6). In cytotoxicity assay, although all three agents induced cell death in a dose and time-dependent manner, paclitaxel and topotecan showed higher IC_{50} values in comparison to previous studies [49–52] which might be attributed to acquired drug resistance in our cells [53,54].

Paclitaxel is a common cancer drug from the taxane family, which interferes with normal function of microtubules during cell division [55]. To date, multiple mechanisms have been proposed for acquired resistance to paclitaxel including overexpression of multidrug transporter genes [56,57], point mutations of beta-tubulin gene [58] and altered expression of certain β-tubulin isotypes [59].

Topotecan is a topoisomerase I inhibitor. This enzyme relaxes the accumulated supercoils in DNA during replication [60]. Therefore, it is possible that cells failing to enter S-phase or replicate DNA during exposure to the drug, would acquire topotecan resistance [61].

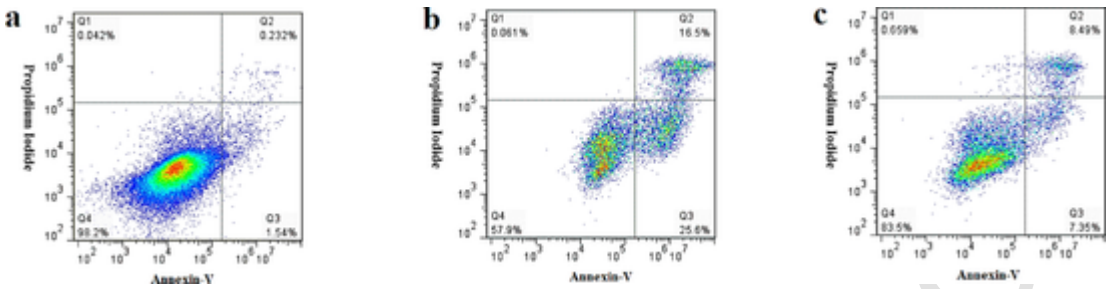

Fig. 9. Quantification of apoptotic cells by FITC-annexin V/PI staining as analyzed by flow cytometry. Dot plot of HeLa cells without treatment (a), treated with cisplatin (b) and 1 (c) for 16 h. Quadrant 4, living cells An^-/PI^-; Quadrant 3, early apoptotic cells An^+/PI^-; Quadrant 2, late apoptotic and necrotic cells An^+/PI^+.

In the next step, different concentrations of the combination of **1** and the three drugs were prepared with constant ratios (Tables 1– 3), according to Chou and Talalay method, and then their effects were investigated on cells. Results of median effect method demonstrated that **1** plus cisplatin, paclitaxel, and topotecan had a synergistic inhibitory effect on cervical cancer cells and in most concentrations the CI was less than 1 (Table 7). These observations are similar to other studies, in which significant synergy was reported between a Cu-complex and chemotherapy drugs on breast and cervical cancer cell lines [62,63]. The greatest observed synergistic effect in this study was obtained after combination of **1** with topotecan at 72 h and in IC_{50}, in which CI = 0.22 and DRI for **1** and topotecan were calculated as 16 and 6.3 folds, respectively. This means that combination of these drugs could allow for a more efficient treatment option, with lower drug dosages and less cytotoxicity; implying potentially fewer side effects. Use of these drugs with synergistic effects at lower concentrations would be more effective and useful for clinical use. However, repeating the experiments on non-resistant cells, would be more informative.

The nature of metal ions, their oxidation states, variable coordination modes, the type and number of bound ligands and reactivity towards the organic substrates can influence the biological activities of metal complexes. These criteria can be considered in design of novel and more potent metal complexes [64]. Recently, Ndagi and his colleagues have reviewed the newly designed metal complexes and their cytotoxic effects on cancer cell lines, as well as various molecular targets in cancer therapy [65].

The molecular mechanisms underlying the anticancer effects of copper complexes were initially investigated with a vision that cisplatin and its analogues bind to DNA. Further studies showed that copper complexes can exert their anticancer effects *via* different mechanisms, including DNA binding, intercalation and cleavage activity, superoxide dismutase (SOD) mimetic activity, as well as generation of reactive oxygen species (ROS). It has been proposed that copper-based compounds are promising candidates for cancer therapy due to their DNA targeting effects, inhibition of topoisomerases and proteasomes. Chakraborty *et al.*, reported that apoptosis in MCF-7 cancer cells was triggered through caspase-3 pathway and inhibition of AKT, and matrix metalloproteinase-9 after treatment with copper complex [66]. Similarly, Qiao *et al.*, demonstrated that Cu complex can induce apoptosis in HeLa cells via activation of caspase-9 and caspase-3 [67]. Moreover, it has been shown that $Cu(SBCM)_2$ induced cell cycle arrest and triggered apoptotic pathway in breast cancer cells by down regulation of mutant P53 and matrix metalloproteinase-2 [68]. Several publications reported that copper complexes were able to inhibit topoisomerases I and II. Effective cytotoxicity of copper complex towards EKY3 cancer cells has been related to topoisomerase I inhibition [69]. Sandhaus *et al.,* synthesized a novel Cu complex and evaluated its anticancer activity towards colon and breast cancer cell lines. Their results indicated that the complex acted as a potent inhibitor of human topoisomerase II [70]. Furthermore, it has been shown that proteasomes are potent molecular targets for Cu complexes. In this regard Chen *et al.*, reported the significant inhibition of prostate tumor is associated with the proteasome inhibition [71]. Li *et al.*, also showed that copper complexes as antitumor agents could inhibit proteasome, accumulate the ubiquitinated proteins and induce apoptosis in breast cancer cells [72]. Finally, these molecular events can lead to cell death through apoptotic pathways [8]. However, the discovery of the exact molecular mechanism(s) of cell death requires further experiments.

Based on this study, **1** displayed significant antiproliferative effects on cancerous cell lines including CT26, C26, TUBO and 4T1 and also anticancer activity on HeLa cells. Similarly, **2** indicated notable toxicity towards both murine and human colon cancer cells. Further studies based on combination chemotherapy approach showed that **1** could be considered as a potent chemotherapeutic agent especially when used in combination with topotecan. However, further studies are required on other cancerous cell lines and animal models to better elucidate its therapeutic effects.

5. Conclusions

In this work, we report an approach in which mixed-ligand strategy with the bioactive metal of copper leads to the formation of two heteroleptic complexes that benefit from extensive intermolecular interactions such as hydrogen bond and π-π interactions. Complexes **1** and **2** are the discrete examples based on the pyridinedicarboxylic acid *N*-oxide ligand which compared with the intact pyridinedicarboxylic acid. The *N*-oxidation form of the ligands has not been much considered in the coordination compounds, so this actually represents the novelty of this work. We have also considered the antiproliferative effects of these complexes in some murine and human cancerous cells. Moreover, combination results revealed the inhibitory effects of **1** on HeLa cell growth which was synergistically enhanced by combination with common chemotherapeutic drugs at certain concentrations and time points. Complex **1** induced apoptosis in HeLa cells and exhibited a profile similar to cisplatin, while it had less toxicity on HDF normal cells. Thus, **1** is suggested as a potent agent to be used in combination with other chemotherapeutic drugs. However, more studies are required to elucidate its exact mechanism(s) both *in vitro* and *in vivo*.

CRediT authorship contribution statement

Hossein S. Moradi: Methodology, Formal analysis, Investigation, Data curation, Writing – original draft. **Elham Momenzadeh:** Methodology, Formal analysis, Investigation, Data curation, Writing – original draft. **Monireh Asar:** Methodology, Formal analysis, Investigation, Data curation, Writing – original draft. **Sonia Iranpour:** Methodology, Formal analysis, Investigation, Data curation, Writing – original draft. **Ahmad Reza Bahrami:** Funding acquisition, Supervision, Writing – review & editing, Project administration, Visualization. **Maryam Bazargan:** Formal analysis, Software, Data curation, Writing – original draft. **Maryam M. Matin:** Funding acquisition, Supervision, Writing – review & editing, Project administra-

tion, Visualization. **Masoud Mirzaei:** Conceptualization, Funding acquisition, Supervision, Writing – review & editing, Project administration, Visualization.

Declaration of Competing Interest

Hereby I declare that we have NO conflict of interest.

Acknowledgements

We would like to thank Mrs. Zahra Hosseini-Hashemi for synthesizing complex **1** and Atefeh Pesaraklou for her great technical help. We are also grateful to Mahdi Mirahmadi for his technical assistance in flow cytometry analysis. This study was financially supported by Ferdowsi University of Mashhad, Mashhad, Iran (Grant numbers 31817/3, 46881, and 45374). This project is funded by Iran Science Elites Federation (Grant No. M/98208, M/99397, and M/400230).

Supplementary materials

Supplementary material associated with this article can be found, in the online version, at doi:10.1016/j.molstruc.2021.131584.

References

[1] A. Jemal, F. Bray, M.M. Center, J. Ferlay, E. Ward, D. Forman, Global cancer statistics, CA, Cancer J. Clin. 61 (2011) 69–90, https://doi.org/10.3322/caac.20107.
[2] E.M. Yonika Arum Larasati, D.D.P. Putri, R.Y. Utomo, A. Hermawan, Combination of cisplatin and cinnamon essential oil inhibits HeLa cells proliferation through cell cycle arrest, J. Appl. Pharm. Sci. 4 (2014) 014–019, https://doi.org/10.7324/JAPS.2014.41203.
[3] H. Joensuu, Systemic chemotherapy for cancer: from weapon to treatment, Lancet Oncol. 9 (2008) 304, https://doi.org/10.1016/S1470-2045(08)70075-5.
[4] I. Ott, R. Gust, Non platinum metal complexes as anti-cancer drugs, Arch. Pharm. (Weinheim). 340 (2007) 117–126, https://doi.org/10.1002/ardp.200600151.
[5] N. Colombo, S. Carinelli, A. Colombo, C. Marini, D. Rollo, C. Sessa, Cervical cancer: ESMO clinical practice guidelines for diagnosis, treatment and follow-up, Ann. Oncol. 23 (2012) vii27-vii32, https://doi.org/10.1093/annonc/mds268.
[6] J. Pontén, H.-O. Adami, R. Bergström, J. Dillner, L.-G. Friberg, L. Gustafsson, A.B. Miller, D.M. Parkin, P. Sparén, D. Trichopoulos, Strategies for global control of cervical cancer, Int. J. Cancer 60 (1995) 1–26, https://doi.org/10.1002/ijc.2910600102.
[7] I. Iakovidis, I. Delimaris, S.M. Piperakis, Copper and its complexes in medicine: a biochemical approach, Mol. Biol. Int. 2011 (2011) 1–13, https://doi.org/10.4061/2011/594529.
[8] C. Marzano, M. Pellei, F. Tisato, C. Santini, Copper complexes as anticancer agents, Anticancer. Agents Med. Chem. 9 (2009) 185–211.
[9] B. Halliwell, J.M. Gutteridge, Role of free radicals and catalytic metal ions in human disease: an overview, Methods Enzymol. 186 (1990) 1–85.
[10] M.C. Linder, Biochemistry of Copper, Springer US, Boston, MA, 1991, https://doi.org/10.1007/978-1-4757-9432-8.
[11] M. Bazargan, M. Mirzaei, A. Franconetti, A. Frontera, On the preferences of five-membered chelate rings in coordination chemistry: insights from the Cambridge Structural Database and theoretical calculations, Dalton Trans. 48 (2019) 5476–5490, https://doi.org/10.1039/C9DT00542K.
[12] E.K. Efthimiadou, H. Thomadaki, Y. Sanakis, C.P. Raptopoulou, N. Katsaros, A. Scorilas, A. Karaliota, G. Psomas, Structure and biological properties of the copper (II) complex with the quinolone antibacterial drug N-propyl-norfloxacin and 2,2′-bipyridine, J. Inorg. Biochem. 101 (2007) 64–73, https://doi.org/10.1016/j.jinorgbio.2006.07.019.
[13] W.R. Greco, H. Faessel, L. Levasseur, The search for cytotoxic synergy between anticancer agents: a case of Dorothy and the Ruby slippers?, J. Natl. Cancer Inst. 88 (1996) 699–700, https://doi.org/10.1093/jnci/88.11.699.
[14] T.C. Chou, Drug combination studies and their synergy quantification using the Chou-Talalay method, Cancer Res 70 (2010) 440–446, https://doi.org/10.1158/0008-5472.CAN-09-1947.
[15] K.R. Roell, D.M. Reif, A.A. Motsinger-Reif, An introduction to terminology and methodology of chemical synergy—Perspectives from across disciplines, Front. Pharmacol. 8 (2017) 158, https://doi.org/10.3389/fphar.2017.00158.
[16] S. Elmore, Apoptosis: a review of programmed cell death, Toxicol. Pathol. 35 (2007) 495–516, https://doi.org/10.1080/01926230701320337.
[17] S.H. Kaufmann, W.C. Earnshaw, Induction of apoptosis by cancer chemotherapy, Exp. Cell Res. 256 (2000) 42–49, https://doi.org/10.1006/excr.2000.4838.
[18] A. Hashemzadeh, G.P.C. Drummen, A. Avan, M. Darroudi, M. Khazaei, R. Khajavian, A. Rangrazi, M. Mirzaei, When metal–organic framework mediated smart drug delivery meets gastrointestinal cancers, J. Mater. Chem. B. 9 (2021) 3967–3982, https://doi.org/10.1039/D1TB00155H.
[19] S. Iranpour, A.R. Bahrami, A. Sh. Saljooghi, M.M. Matin, Application of smart nanoparticles as a potential platform for effective colorectal cancer therapy, Coord. Chem. Rev. 442 (2021) 213949, https://doi.org/10.1016/j.ccr.2021.213949.
[20] Z.H. Hashemi, M. Mirzaei, H. Eshtiagh-Hosseini, F. Sadeghi, M. Shamsipur, M. Ardalani, A.J. Blake, Solid and solution states studies of two Mn(II) complexes based on N -oxidized pyridine-2,5-dicarboxylic acid, J. Coord. Chem. 71 (2018) 4058–4071, https://doi.org/10.1080/00958972.2018.1539712.
[21] L. Syper, K. Kloc, J. Mz.xl;lochowski, Synthesis of ubiquinone and menaquinone analogues by oxidative demethylation of alkenylhydroquinone ethers with argentic oxide or ceric ammonium nitrat, Tetrahedron 36 (1980) 123–129, https://doi.org/10.1016/0040-4020(80)85034-4.
[22] Z. Hosseini-Hashemi, M. Mirzaei, A. Jafari, P. Hosseinpour, M. Yousefi, A. Frontera, M.L. Dashtbayaz, M. Shamsipur, M. Ardalani, Effects of N -oxidation on the molecular and crystal structures and properties of isocinchomeronic acid, its metal complexes and their supramolecular architectures: experimental, CSD survey, solution and theoretical approaches, RSC Adv 9 (2019) 25382–25404, https://doi.org/10.1039/C9RA05143K.
[23] H. Brandenburg, K. Putz, DIAMOND, Crystal Impact GbR, Bonn, Germany. (2012).
[24] S. APEX2 and SAINT, No Title, Bruker AXS LLC, Madison, WI, 2020. (2020).
[25] L. Krause, R. Herbst-Irmer, G.M. Sheldrick, D. Stalke, Comparison of silver and molybdenum microfocus X-ray sources for single-crystal structure determination, J. Appl. Crystallogr. 48 (2015) 3–10, https://doi.org/10.1107/S1600576714022985.
[26] G.M. Sheldrick, SHELXT–Integrated space-group and crystal-structure determination, Acta Cryst. A71 (2015) 3–8, https://doi.org/10.1107/S2053273314026370.
[27] G.M. Sheldrick, Crystal structure refinement with SHELXL, Acta Cryst. C 71 (2015) 3–8, https://doi.org/10.1107/S2053229614024218.
[28] T. Mosmann, Rapid colorimetric assay for cellular growth and survival: application to proliferation and cytotoxicity assays, J. Immunol. Methods 65 (1983) 55–63, https://doi.org/10.1016/0022-1759(83)90303-4.
[29] M. Mirzaei, F. Sadeghi, K. Molčanov, J.K. Zaręba, R.M. Gomila, A. Frontera, Recurrent supramolecular motifs in a series of Acid–Base adducts based on Pyridine-2,5-Dicarboxylic Acid N -Oxide and organic bases: inter and intramolecular hydrogen bonding, Cryst. Growth Des. 20 (2020) 1738–1751, https://doi.org/10.1021/acs.cgd.9b01475.
[30] M. Bazargan, M. Mirzaei, M. Aghamohamadi, M. Tahmasebi, A. Frontera, Supramolecular assembly of a 2D coordination polymer bearing pyridine-N-oxide-2,5-dicarboxylic acid and copper ion: X-ray crystallography and DFT calculations, J. Mol. Struct. 1202 (2020) 127243, https://doi.org/10.1016/j.molstruc.2019.127243.
[31] M. Bazargan, M. Mirzaei, H. Eshtiagh-Hosseini, J.T. Mague, A. Bauzá, A. Frontera, Synthesis, X-ray characterization and DFT study of a novel Fe(III)–pyridine-2,6-dicarboxylic acid N -oxide complex with unusual coordination mode, Inorg. Chim. Acta 449 (2016) 44–51, https://doi.org/10.1016/j.ica.2016.04.044.
[32] M. Mirzaei, H. Eshtiagh-Hosseini, M. Bazargan, F. Mehrzad, M. Shahbazi, J.T. Mague, A. Bauzá, A. Frontera, Two new copper and nickel complexes of pyridine-2,6-dicarboxylic acid N-oxide and their proton transferred salts: Solid state and DFT insights, Inorg. Chim. Acta 438 (2015) 135–145, https://doi.org/10.1016/j.ica.2015.08.030.
[33] M. Shahbazi, F. Mehrzad, M. Mirzaei, H. Eshtiagh-Hosseini, J.T. Mague, M. Ardalani, M. Shamsipur, Synthesis, single crystal X-ray characterization, and solution studies of Zn(II)-, Cu(II)-, Ag(I)- and Ni(II)-pyridine-2,6-dipicolinate N-oxide complexes with different topologies and coordination modes, Inorg. Chim. Acta. 458 (2017) 84–96, https://doi.org/10.1016/j.ica.2016.12.030.
[34] M. Mirzaei, H. Eshtiagh-Hosseini, M. Bazargan, Syntheses and X-ray crystal structure studies of four new coordination complexes and salts based on proton-transferred pyridine-2,6-dicarboxylic acid N-oxide, Res. Chem. Intermed. 41 (2015) 9785–9803, https://doi.org/10.1007/s11164-015-1965-x.
[35] M. Ataei, V. Jodaeian, M. Mirzaei, A. Sh. Saljooghi, A. Gholizadeh, Syntheses, characterization, and antiproliferative study of some complexes containing pyridine-2,6-dicarboxylic acid N-oxide, Nashrieh Shimi va Mohandesi Shimi Iran (2019) http://www.nsmsi.ir/article_36163.html.
[36] K. Nakamoto, Infrared and Raman spectra of inorganic and coordination compounds, in: P.R. Griffiths (Ed.), Handb. Vib. Spectrosc., John Wiley & Sons, Ltd, Chichester, UK, 2006, pp. 1872–1892, https://doi.org/10.1002/0470027320.s4104.
[37] J.F. Kerr, A.H. Wyllie, A.R. Currie, Apoptosis: a basic biological phenomenon with wide-ranging implications in tissue kinetics, Br. J. Cancer. 26 (1972) 239–257.
[38] BioLegend, FITC Annexin V Apoptosis Detection Kit with PI, (2017).
[39] U. Jungwirth, C.R. Kowol, B.K. Keppler, G. Christian, Anticancer activity of metal complexes : involvement of redox processes, Antioxid. Redox Signal 15 (2012) 1085–1127, https://doi.org/10.1089/ars.2010.3663.Anticancer.
[40] B. Rosenberg, L. VanCamp, J.E. Trosko, V.H. Mansour, Platinum compounds: a new class of potent antitumour agents, Nature 222 (1969) 385–386.
[41] S. Dasari, P.B. Tchounwou, Cisplatin in cancer therapy: molecular mechanisms of action, Eur. J. Pharmacol. 740 (2014) 364–378, https://doi.org/10.1016/j.ejphar.2014.07.025.
[42] S. van Zutphen, J. Reedijk, Targeting platinum anti-tumour drugs: overview of strategies employed to reduce systemic toxicity, Coord. Chem. Rev. 249 (2005) 2845–2853, https://doi.org/10.1016/j.ccr.2005.03.005.
[43] T.S. Kamatchi, N. Chitrapriya, H. Lee, C.F. Fronczek, F.R. Fronczek, K. Natarajan, Ruthenium(II)/(III) complexes of 4-hydroxy-pyridine-2,6-dicarboxylic acid with PPh3/AsPh3 as co-ligand: Impact of oxidation state and co-ligands on anticancer activity in vitro, Dalton Trans 41 (2012) 2066–2077, https://doi.org/10.1039/C1DT11273B.
[44] T.S. Kamatchi, N. Chitrapriya, V.S. Jamal Ahamed, S.-S. Moon, F.R. Fronczek, K.

Natarajan, Ruthenium(II) complexes of 2,2′-bipyridine-5,5′-dicarboxylic acid: synthesis, structure, DNA binding, cytotoxicity and antioxidant activity, Inorg. Chim. Acta 404 (2013) 58–67, https://doi.org/10.1016/j.ica.2013.04.029.
[45] R.C. HARRISON, C.A. MCAULIFFE, A.M. ZAKI, ChemInform abstract: an efficient route for the preparation of highly soluble platinum(II) antitumor agents, Chem. Informationsd 11 (1980). 10.1002/chin.198022299.
[46] M. Galanski, B. Keppler, Carboxylation of dihydroxoplatinum (IV) complexes via a new synthetic pathway, Inorg. Chem. (1996) 1709–1711.
[47] C.M. Giandomenico, M.J. Abrams, B.A. Murrer, J.F. Vollano, M.I. Rheinheimer, S.B. Wyer, G.E. Bossard, J.D. Higgins, Carboxylation of kinetically inert Platinum(IV) hydroxy complexes. an entr.acte.ee into orally active Platinum(IV) antitumor agents, Inorg. Chem. 34 (1995) 1015–1021, https://doi.org/10.1021/ic00109a004.
[48] D.-Y. Lu, T.-R. Lu, J. Ding, B. Xu, J.-Y. Che, H.-Y. Wu, Anticancer drug sensitivity testing, a historical review and future perspectives, Curr. Drug Ther. 10 (2015) 44–55, https://doi.org/10.2174/1574885510011508251004 50.
[49] J. Liebmann, J. Cook, C. Lipschultz, D. Teague, J. Fisher, J. Mitchell, Cytotoxic studies of paclitaxel (Taxol®) in human tumour cell lines, Br. J. Cancer 68 (1993) 1104–1109, https://doi.org/10.1038/bjc.1993.488.
[50] E.Y. Chi, B. Viriyapak, H.S. Kwack, Y.K. Lee, S. Il Kim, K.H. Lee, T.C. Park, Regulation of paclitaxel-induced programmed cell death by autophagic induction: A model for cervical cancer, Obstet. Gynecol. Sci. 56 (2013) 84, https://doi.org/10.5468/OGS.2013.56.2.84.
[51] W. Bi, Y. Wang, G. Sun, X. Zhang, Y. Wei, L. Li, X. Wang, Paclitaxel-resistant HeLa cells have up-regulated levels of reactive oxygen species and increased expression of taxol resistance gene 1, Pak. J. Pharm. Sci. 27 (2014) 871–878 http://www.ncbi.nlm.nih.gov/pubmed/25015454.
[52] U. Serbes, O.D. Ozsoylemez, G. Ozcan, Evaluation of Paclitaxel effects in the pattern of expression of survival and apoptotic genes regulators in HeLa cells, Curr. Pharm. Biotechnol. 17 (2016) 1058–1067, https://doi.org/10.2174/1389201017666160914190550.
[53] K. Takara, T. Sakaeda, T. Yagami, H. Kobayashi, N. Ohmoto, M. Horinouchi, K. Nishiguchi, K. Okumura, Cytotoxic effects of 27 anticancer drugs in HeLa and MDR1-overexpressing derivative cell lines, Biol. Pharm. Bull. 25 (2002) 771–778, https://doi.org/10.1248/bpb.25.771.
[54] J. Zhang, J. Zhao, W. Zhang, G. Liu, D. Yin, J. Li, S. Zhang, H. Li, Establishment of Paclitaxel-resistant cell line and the underlying mechanism on drug resistance, Int. J. Gynecol. Cancer. 1 (2012), https://doi.org/10.1097/IGC.0b013e31826e2382.
[55] M. Shimomura, T. Yaoi, K. Itoh, D. Kato, K. Terauchi, J. Shimada, S. Fushiki, Drug resistance to paclitaxel is not only associated with ABCB1 mRNA expression but also with drug accumulation in intracellular compartments in human lung cancer cell lines, Int. J. Oncol. 40 (2012) 995–1004, https://doi.org/10.3892/ijo.2011.1297.
[56] J.T. Lee, L.S. Steelman, J.A. McCubrey, Phosphatidylinositol 3′-kinase activation leads to multidrug resistance protein-1 expression and subsequent chemoresistance in advanced prostate cancer cells, Cancer Res. 64 (2004) 8397–8404, https://doi.org/10.1158/0008-5472.CAN-04-1612.
[57] H. Wang, T. Vo, A. Hajar, S. Li, X. Chen, A.M. Parissenti, D.N. Brindley, Z. Wang, Multiple mechanisms underlying acquired resistance to taxanes in selected docetaxel-resistant MCF-7 breast cancer cells, BMC Cancer 14 (2014) 1–15, https://doi.org/10.1186/1471-2407-14-37.
[58] P. Giannakakou, D.L. Sackett, Y.K. Kang, Z. Zhan, J.T.M. Buters, T. Fojo, M.S. Poruchynsky, Paclitaxel-resistant human ovarian cancer cells have mutant β-tubulins that exhibit impaired paclitaxel-driven polymerization, J. Biol. Chem. 272 (1997) 17118–17125, https://doi.org/10.1074/jbc.272.27.17118.
[59] D. Aoki, Y. Oda, S. Hattori, K.I. Taguchi, Y. Ohishi, Y. Basaki, S. Oie, N. Suzuki, S. Kono, M. Tsuneyoshi, M. Ono, T. Yanagawa, M. Kuwano, Overexpression of class III β-tubulin predicts good response to taxane-based chemotherapy in ovarian clear cell adenocarcinoma, Clin. Cancer Res. 15 (2009) 1473–1480, https://doi.org/10.1158/1078-0432.CCR-08-1274.
[60] B.L. Staker, K. Hjerrild, M.D. Feese, C.A. Behnke, A.B. Burgin, L. Stewart, Nonlinear partial differential equations and applications: The mechanism of topoisomerase I poisoning by a camptothecin analog, Proc. Natl. Acad. Sci. 99 (2002) 15387–15392, https://doi.org/10.1073/pnas.242259599.
[61] I. Chourpa, J.-M. Millot, G.D. Sockalingum, J.-F. Riou, M. Manfait, Kinetics of lactone hydrolysis in antitumor drugs of camptothecin series as studied by fluorescence spectroscopy, Biochim. Biophys. Acta Gen. Subj. 1379 (1998) 353–366, https://doi.org/10.1016/S0304-4165(97)00115-3.
[62] G. Geromichalos, G. Katsoulos, C. Hadjikostas, K. AH, D. Kyriakidis, In vitro combination effect of a new series of copper(II) complexes with cisplatin or epirubicin on human breast and cervical cancer cell lines, Drugs Exp. Clin. Res. 24 (1998) 93–104.
[63] G.D. Geromichalos, G.A. Katsoulos, D.T. Trafalis, C.C. Hadjikostas, A. Papageorgiou, Synergistic interaction between a novel mixed ligand copper(II) chelate complex and a panel of anticancer agents in T47D human breast cancer cells in vitro, J. Buon. 11 (2006) 469–476.
[64] M. Frezza, S. Hindo, D. Chen, A. Davenport, S. Schmitt, D. Tomco, Q.P. Dou, Novel metals and metal complexes as platforms for cancer therapy, Curr. Pharm. Des. 16 (2010) 1813–1825, https://doi.org/10.2174/138161210791209009.
[65] U. Ndagi, N. Mhlongo, M. Soliman, Metal complexes in cancer therapy – an update from drug design perspective, Drug Des. Devel. Ther. 11 (2017) 599–616, https://doi.org/10.2147/DDDT.S119488.
[66] A. Chakraborty, P. Kumar, K. Ghosh, P. Roy, Evaluation of a Schiff base copper complex compound as potent anticancer molecule with multiple targets of action, Eur. J. Pharmacol. 647 (2010) 1–12.
[67] X. Qiao, Z.-Y. Ma, C.-Z. Xie, F. Xue, Y.-W. Zhang, J.-Y. Xu, Z.-Y. Qiang, J.-S. Lou, G.-J. Chen, S.-P. Yan, Study on potential antitumor mechanism of a novel Schiff Base copper (II) complex: synthesis, crystal structure, DNA binding, cytotoxicity and apoptosis induction activity, J. Inorg. Biochem. 105 (2011) 728–737.
[68] J.B. Foo, M.L. Low, J.H. Lim, Y.Z. Lor, R.Z. Abidin, V.E. Dam, N.A. Rahman, C.Y. Beh, L.C. Chan, C.W. How, Copper complex derived from S-benzyldithiocarbazate and 3-acetylcoumarin induced apoptosis in breast cancer cell, BioMetals 31 (2018) 505–515.
[69] S. Castelli, M.B. Goncalves, P. Katkar, G.C. Stuchi, R.A.A. Couto, H.M. Petrilli, A.M. da Costa Ferreira, Comparative studies of oxindolimine-metal complexes as inhibitors of human DNA topoisomerase IB, J. Inorg. Biochem. 186 (2018) 85–94.
[70] S. Sandhaus, R. Taylor, T. Edwards, A. Huddleston, Y. Wooten, R. Venkatraman, R.T. Weber, A. González-Sarrías, P.M. Martin, P. Cagle, A novel copper (II) complex identified as a potent drug against colorectal and breast cancer cells and as a poison inhibitor for human topoisomerase IIα, Inorg. Chem. Commun. 64 (2016) 45–49.
[71] D. Chen, Q.C. Cui, H. Yang, R.A. Barrea, F.H. Sarkar, S. Sheng, B. Yan, G.P.V. Reddy, Q.P. Dou, Clioquinol, a therapeutic agent for Alzheimer's disease, has proteasome-inhibitory, androgen receptor–suppressing, apoptosis-inducing, and antitumor activities in human prostate cancer cells and xenografts, Cancer Res 67 (2007) 1636–1644.
[72] D.D. Li, E. Yagüe, L.Y. Wang, L.L. Dai, Z.B. Yang, S. Zhi, N. Zhang, X.-M. Zhao, Y.H. Hu, Novel copper complexes that inhibit the proteasome and trigger apoptosis in triple-negative breast cancer cells, ACS Med. Chem. Lett. 10 (2019) 1328–1335.